THE JOURNAL OF BIOLOGICAL CHEMISTRY VOL. 286, NO. 4, pp. 2774–2784, January 28, 2011

Product-assisted Catalysis as the Basis of the Reaction Specificity of Threonine Synthase*[S]

Received for publication, September 17, 2010, and in revised form, October 27, 2010 Published, JBC Papers in Press, November 17, 2010, DOI 10.1074/jbc.M110.186205

Takeshi Murakawa, Yasuhiro Machida, and Hideyuki Hayashi[1]

From the Department of Biochemistry, Faculty of Medicine, Osaka Medical College, Takatsuki 569-8686, Japan

Threonine synthase (TS), which is a pyridoxal 5′-phosphate (PLP)-dependent enzyme, catalyzes the elimination of the γ-phosphate group from *O*-phospho-L-homoserine (OPHS) and the subsequent addition of water at Cβ to form L-threonine. The catalytic course of TS is the most complex among the PLP enzymes, and it is an intriguing problem how the elementary steps are controlled in TS to carry out selective reactions. When L-vinylglycine was added to *Thermus thermophilus* HB8 TS in the presence of phosphate, L-threonine was formed with k_{cat} and reaction specificity comparable with those when OPHS was used as the substrate. However, in the absence of phosphate or when sulfate was used in place of phosphate, only the side reaction product, α-ketobutyrate, was formed. Global analysis of the spectral changes in the reaction of TS with L-threonine showed that compared with the more acidic sulfate ion, the phosphate ion decreased the energy levels of the transition states of the addition of water at the Cβ of the PLP-α-aminocrotonate aldimine (AC) and the transaldimination to form L-threonine. The x-ray crystallographic analysis of TS complexed with an analog for AC gave a distinct electron density assigned to the phosphate ion derived from the solvent near the Cβ of the analog. These results indicated that the phosphate ion released from OPHS by γ-elimination acts as the base catalyst for the addition of water at Cβ of AC, thereby providing the basis of the reaction specificity. The phosphate ion is also considered to accelerate the protonation/deprotonation at Cγ.

Threonine synthase (TS)[2] catalyzes the last step of the L-threonine biosynthesis, conversion of *O*-phospho-L-homoserine (OPHS) into L-threonine and inorganic phosphate (1). TS is a pyridoxal 5′-phosphate (PLP)-dependent enzyme and, together with the L- and D-serine dehydratases, threonine dehydratase, tryptophan synthase, and cysteine synthase, constitutes the β-family of PLP enzymes (2, 3). Structurally, these enzymes form fold type II PLP enzymes (4). Because TS is found only in bacteria (5), yeasts (6), and plants (4, 7), it can be a target for developing antibacterial drugs (5). For this purpose, elucidation of the mechanism of action of TS is crucial.

The reaction mechanism of TS is considered to be the most complicated one catalyzed by the PLP enzymes, proceeding through all the types of intermediates formed during the catalysis of the PLP enzymes (summarized in Scheme 1 (1, 3, 8, 9)). In this mechanism, OPHS reacts with the PLP-Lys aldimine (internal aldimine **1**) to form the external aldimine (**2**) and liberates the side chain of the Lys residue (transaldimination). The intermediate **2** is then converted to the ketimine (**3**) via a 1,3-prototropic shift. The electron-withdrawing imino group promotes deprotonation at Cβ, and after the formation of the enamine (**4**), the γ-phosphate group is eliminated, yielding β,γ-unsaturated ketimine (**5**) and a phosphate ion. In **5**, deprotonation at C4′ of the cofactor and protonation at Cγ of the substrate moiety occur to form the PLP-α-aminocrotonate aldimine, **6**). The stereospecific addition of a water molecule from the *Re* face (Cβ being taken as the prochiral center) of **6** to the Cα-Cβ double bond yields the PLP-L-threonine aldimine (**8**) via the quinonoid intermediate (**7**). Finally, attack of the ϵ-amino group of Lys on **8** releases the product L-threonine and regenerates the internal aldimine (**1**).

The remarkable feature of this catalytic reaction is that TS can carry out many regiospecific (C4′, Cα, Cβ, and Cγ) and stereospecific proton transfers at the coenzyme-substrate complexes. Therefore, it is an intriguing problem how such specific proton transfers are enabled to optimize the reaction specificity of TS.

To provide a structural basis for resolving this issue, we previously determined the x-ray crystallographic structures of a thermostable TS from *Thermus thermophilus* HB8 in the unliganded form and a complex form with the substrate analog, 2-amino-5-phosphonopentanoic acid (AP5) (8). The structure of the complex with AP5 showed an sp^2 hybridization configuration at Cα and Cβ and an sp^3 hybridization configuration at C4′, indicating that it is an enamine analogous to **4**. In this structure, the ϵ-amino N of Lys-61 is 3.5, 3.3, and 3.6 Å away from C4′, Cα, and Cβ, respectively. Considering the fact that the PLP binding lysine residue is the general base catalyst for the 1,3-prototropic shift in aminotransferases (10), we can expect that the ϵ-amino group of Lys-61 is the general base catalyst for the protonation/deprotonation at these atoms, which is involved in steps **2**–**3**, **3**–**4**, and **7**–**8**.

* This work was supported in part by Grants-in-aid for Scientific Research 21570120 (to H. H.) and 91445990 (to T. M.) from the Japan Society for the Promotion of Science.

[S] The on-line version of this article (available at http://www.jbc.org) contains supplemental Figs. S2–S3.

The atomic coordinates and structure factors (codes 3AEY and 3AEX) have been deposited in the Protein Data Bank, Research Collaboratory for Structural Bioinformatics, Rutgers University, New Brunswick, NJ (http://www.rcsb.org/).

[1] To whom correspondence should be addressed: Dept. of Biochemistry, Faculty of Medicine, Osaka Medical College, 2-7 Daigakumachi, Takatsuki 569-8686, Japan. Fax: 81-72-684-6516; E-mail: hayashi@art.osaka-med.ac.jp.

[2] The abbreviations used are: TS, threonine synthase; OPHS, *O*-phospho-L-homoserine; AP5, 2-amino-5-phosphonopentanoic acid; **10**, (*E*)-4-(3-hydroxy-2-methyl-5-(phosphonooxymethyl)pyridin-4-yl)-2-oxobut-3-enoic acid.

In contrast to these steps, however, the catalytic steps involving protonation/deprotonation at Cγ are difficult to understand. The ϵ-amino N of Lys-61 is too far (4.7 Å) from Cγ to directly catalyze the protonation/deprotonation at Cγ, and no appropriate protein side chains that can donate/accept a proton are found in the proximity of Cγ. Based on the crystal structure of the *T. thermophilus* HB8 TS complexed with AP5, we pointed out the possibility that the phosphate released during **4** → **5** may reside at the active site and act as a base catalyst for the protonation/deprotonation at Cγ (8). However, the involvement of the phosphate ion in the proton transfer steps and the reaction specificity of TS have not been experimentally studied.

In this study we performed kinetic and spectroscopic analyses of the reactions of the *T. thermophilus* HB8 TS with OPHS, L-vinylglycine, L-threonine in the presence or absence of phosphate or sulfate and showed that the phosphate ion functions as the catalyst for the addition of water at the Cβ of the PLP-α-aminocrotonate aldimine, thus enabling TS to undergo the β-synthase reaction rather than the γ-lyase reaction. Additionally, the phosphate was also suggested as the catalyst for the protonation/deprotonation at Cγ.

EXPERIMENTAL PROCEDURES

Materials—The recombinant TS was isolated and purified as previously described (8). All other chemicals were of the highest grade commercially available. (*E*)-4-(3-hydroxy-2-methyl-5-(phosphonooxymethyl)pyridin-4-yl)-2-oxobut-3-enoic acid (**10**) was synthesized according to the method of Schnackerz *et al.* (11). Removal of the cofactor from TS was performed by precipitation with ammonium sulfate at low pH according to the method of Toney and Kirsch (10) except that a 100-fold molar excess of hydroxylamine was added to the enzyme to remove PLP from the Lys residue before the addition of ammonium sulfate. The apoenzyme preparation was passed through a PD-10 (GE Healthcare) column twice to remove ammonium sulfate. The concentration of sulfate in the final preparation, measured after heat denaturation (3 min in boiling water) of the protein, was below the detection limit (1 μM) of the photometric method using bromthymol blue (12).

Enzymatic Formation of L-Threonine—TS was incubated with various concentrations of OPHS in a final volume of 100 μl of 50 mM PIPES, 100 mM KCl, 0.1 mM EDTA, pH 8.0. After incubation at 298 K for various periods, 100 μl of 100 mM perchloric acid was added to terminate the reaction. A 100-μl aliquot of 100 mM phenyl isothiocyanate and 100 μl of 1 M triethylamine were then added. After incubation for 1 h at 298 K, 400 μl of hexane was added and mixed, and the lower layer was loaded onto a Wakosil PTC column (Wako, Japan) using a Beckman System Gold analyzer. The phenylthiocarbamyl L-threonine was detected by monitoring the absorbance at 254 nm.

Enzymatic Formation of α-Ketobutyrate—The method used was a modification of that described by Möckel *et al.* (13). Briefly, TS was incubated with each concentration of substrate in a final volume of 1 ml of 50 mM PIPES, 100 mM KCl, 0.1 mM EDTA, pH 8.0. After incubation at 298 K for 1 h, 1 ml of reagent (1 g of semicarbazide HCl plus 0.9 g of sodium acetate in 100 ml of H_2O) was added to terminate the reaction. After incubation for 15 min at 298 K, 3 ml of H_2O was added, and the absorbance due to the semicarbazone was read at 254 nm. Steady-state kinetic parameters were determined by systematically changing the concentration of L-threonine, phosphate, or sulfate. The kinetic data were fitted to the Michaelis-Menten equation by nonlinear regression using KaleidaGraph (Version 3.0, Synergy Software).

Spectrophotometric Measurement—The absorption spectra were measured at 298 K using a Hitachi (Japan) U-3300 spectrophotometer. Stopped-flow spectrophotometry was performed using an Applied Photophysics SX.18MV spectrophotometer. Typically, equal volumes (75 μl each) of solution A (28 μM enzyme and 100 mM phosphate or sulfate) and solution B (various concentrations of L-threonine) were mixed. The mixing dead time was 2.3 ms under an N_2 gas pressure of 500 kPa. The time-resolved spectra were collected at 298 K using SX.18MV equipped with a photodiode array accessory and XScan (Version 1.0, Applied Photophysics). The spectral data were analyzed by ProKineticist II (Version 1.9, Applied Photophysics) to obtain the spectra of the reaction intermediates and the kinetic parameters. The buffer solution for the spectrophotometric measurements contained 50 mM PIPES, 100 mM KCl, 0.1 mM EDTA, pH 8.0. TS was equilibrated with this buffer by gel filtration using a PD-10 column before the measurements.

Crystallization, Data Collection, and Refinement—The apoenzyme of TS was crystallized by the microdialysis method. The enzyme solution (8 mg/ml) was placed in a 50-μl dialysis button and dialyzed at 293 K against 1.45 M ammonium sulfate in 0.1 M MES, pH 6.5. Single crystals with the approximate dimensions of 0.1 × 0.1 × 0.1 mm grew in about 2 weeks, and then the dialysis buttons were transferred to a new reservoir solution supplemented with 40% (v/v) glycerol as a cryoprotectant and kept at 293 K for 5 h. The complex of TS with **10** was crystallized by the hanging drop vapor diffusion method. The drop was composed of 5 μl of protein solution (8 mg/ml apoenzyme in 5 mM Tris-HCl, pH 6.2), 5 μl of reservoir solution (10% (v/v) PEG3350 in 0.1 M Na_2HPO_4 and KH_2PO_4, pH 6.2), and 1 μl of 10 mM **10**. Single crystals with the approximate dimensions of 0.2 × 0.1 × 0.1 mm were obtained by equilibration of the mixture solution against the reservoir solution at 293 K for about 1 week. The crystal was soaked for 10 s in a new reservoir solution supplemented with 30% (v/v) glycerol as a cryoprotectant. The crystals were mounted on thin nylon loops (ø, 0.2–0.3 mm) and frozen by flash-cooling to 100 K in a cold N_2 gas stream. The x-ray diffraction data were collected at 100 K by synchrotron X-radiation (λ = 0.9 Å) using a DIP6040 detector (Bruker AXS, Madison, WI) in the station BL44XU at SPring-8 (Hyogo, Japan). The diffraction data collected for these crystals were processed and scaled using HKL2000 (14). Both crystals belong to the space group $P3_221$. The details and statistics of the data collection are summarized in Table 4. The programs used for the refinements, calculation of the electron-density maps, and assignment of the solvent molecules were CCP4 program suite Version 6.12 (15) and CNS Version 1.2 (16). Manual re-

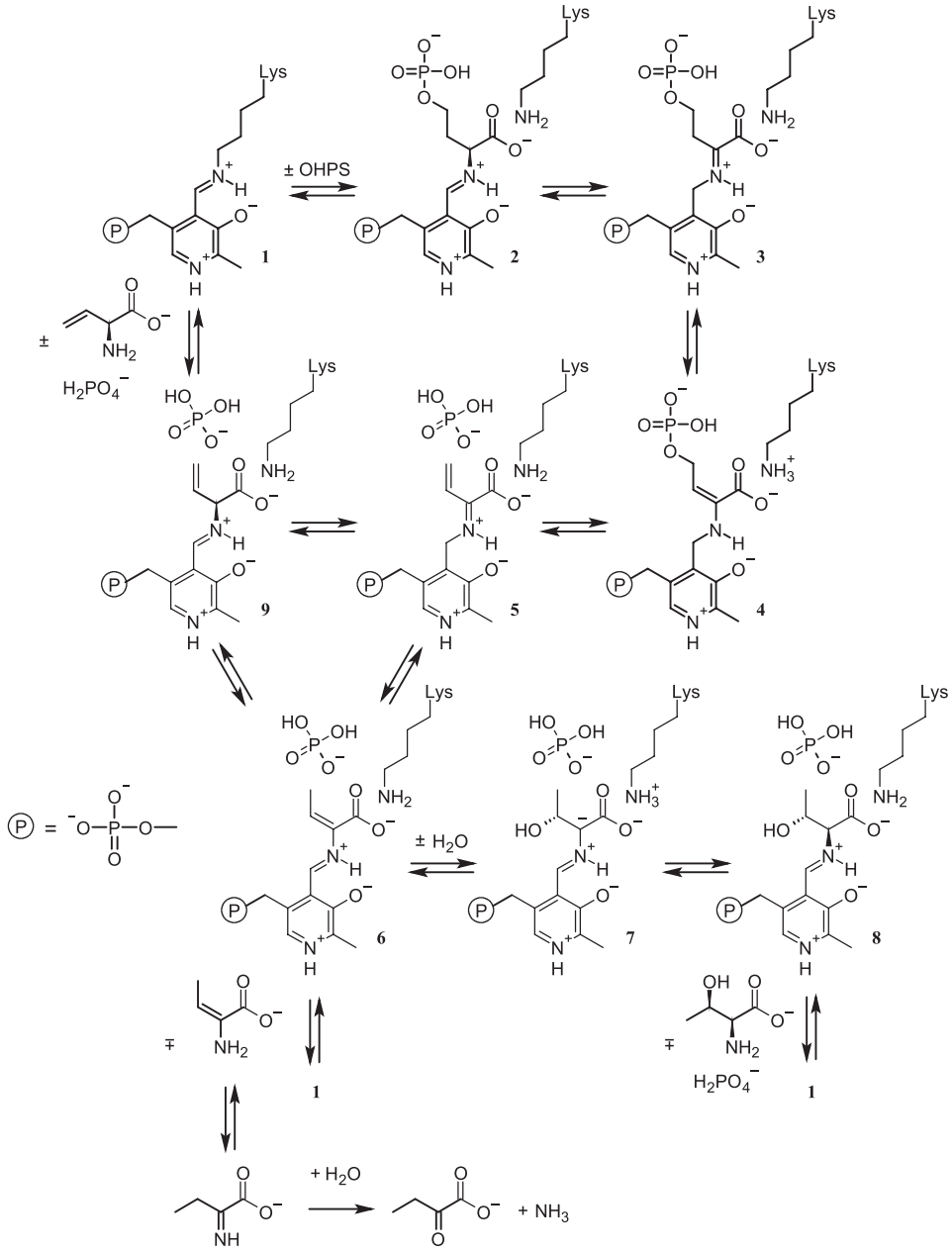

SCHEME 1. **The reaction mechanism of TS.** There is an ambiguity as to the protonation state of the pyridine N1 of the PLP moiety. In this scheme, all the structures were assumed to be protonated at N1. The intermediate **7** is generally called the quinonoid intermediate for its other resonance structure.

building was performed using the Xfit module of the XtalView software package (17). The structure of TS in the holoenzyme form (PDB code 1UIN, Ref. 8) and the structure of TS complexed with AP5 (PDB code 1V7C, Ref. 8) were used as the initial model for the apoenzyme of TS and the TS complexed with **10**, respectively. After being subjected to the rigid-body refinement, the initial structures of the apoenzyme and the complex with **10** were further refined through simulated annealing from 3000 K and several cycles of *B*-factor and positional refinements. The model of **10** was built using MOE Version 2007.09 (Chemical Computing Group), and then the topology and parameter files for refinement in CNS were generated with XPLO2D in the X-UTIL package (18). Water molecules, phosphate ion derived from the reservoir solution, and residues in the active-site region were examined using $2F_o - F_c$, $F_o - F_c$, and omit maps. These models were refined through several additional cycles of the *B*-factor and positional refinements after introducing solvent molecules. The details and statistics of the crystallographic refinement are also summarized in Table 4. The coordinates for the apoenzyme and TS complexed with **10** have been deposited in the PDB with accession codes 3AEY and 3AEX, respectively.

RESULTS

Catalytic Reaction of TS with OPHS and L-Vinylglycine—TS catalyzes the formation of L-threonine from OPHS as a physiological reaction (**1** → **2** → **3** → **4** → **5** → **6** → **7** → **8** → **1** in Scheme 1). In addition, TS catalyzes the formation of α-ketobutyrate from OPHS as a side reaction (**1** → **2** → **3** → **4** → **5** → **6** → **1**). The k_{cat} and k_{cat}/K_m values for the L-threo-

TABLE 1

L-Threonine and α-ketobutyrate formation by TS from OPHS and L-vinylglycine

TS was incubated with various compounds, and the solutions were analyzed for L-threonine and α-ketobutyrate (see "Experimental Procedures"). Values in parentheses are s.d.

Substrate	Phosphate or sulfate[a]	L-Threonine formation		α-Ketobutyrate formation		Reaction specificity[b]	
		k_{cat}	k_{cat}/K_m	k_{cat}	k_{cat}/K_m	k_{cat}	k_{cat}/K_m
		s^{-1}	$M^{-1}s^{-1}$	s^{-1}	$M^{-1}s^{-1}$	%	
OPHS		0.80 (0.03)	5200 (700)	0.0069 (0.0012)	28 (6)	99	99
L-Vinylglycine		—[c]	—	0.015 (0.0002)	0.37 (0.004)	~0	~0
L-Vinylglycine	Phosphate	0.61 (0.12)	5.9 (0.5)	0.013 (0.0006)	0.13 (0.001)	98	98
L-Vinylglycine	Sulfate	—	—	0.0034 (0.0023)	0.037 (0.010)	~0	~0

[a] Concentrations were 50 mM.
[b] Reaction specificity was calculated as (value for the L-threonine formation)/(sum of the values for the L-threonine formation and the α-ketobutyrate formation).
[c] Not detected.

nine formation were about 120- and 190-fold higher, respectively, than those for the α-ketobutyrate formation, yielding a high reaction specificity of 99% in both the k_{cat} and k_{cat}/K_m terms (Table 1). That the ratio of the k_{cat} values for the L-threonine and the α-ketobutyrate formation is similar to the corresponding ratio of the k_{cat}/K_m values is considered to reflect the fact that L-threonine and α-ketobutyrate are derived from the same intermediate bound to the enzyme, *i.e.* the PLP-α-aminocrotonate aldimine (**6**).

A chemical consideration predicts that besides the physiological substrate OPHS, TS may also catalyze the formation of L-threonine from L-vinylglycine via **9** → **6** → **7** → **8**. In this context, the reaction of TS using L-vinylglycine was followed. However, no formation of L-threonine was observed, whereas the side reaction product α-ketobutyrate was formed with a k_{cat} similar to that when OPHS was used as the substrate (Table 1). This indicates that the formation of **6** alone is not enough for producing L-threonine.

During the reaction of TS with OPHS, a phosphate ion is released (**4** → **5**) before the formation of **6** (Scheme 1). To investigate whether the released phosphate ion is involved in the catalysis, the reaction starting from L-vinylglycine was studied in the presence of phosphate and its analog sulfate, which has a similar shape and size as phosphate but has a much lower pK_a value (1.92 at 298 K). In the presence of 50 mM phosphate, L-threonine was preferentially formed (Table 1). In both the k_{cat} and k_{cat}/K_m terms, the reaction specificity was 98%. This is the same pattern as that observed when OPHS was used as the substrate and again reflects the mechanism that L-threonine and α-ketobutyrate are derived from the same intermediate (**6**) bound to the enzyme. The k_{cat} values for the L-threonine and α-ketobutyrate formation were similar to those when OPHS was used as the substrate (Table 1). On the other hand, the k_{cat}/K_m values for the L-threonine and α-ketobutyrate formation were several hundred-fold lower than the corresponding values using OPHS as the substrate (Table 1). This indicates that L-vinylglycine is far more weakly bound to TS than OPHS. According to the previous crystallographic study of TS complexed with AP5 (8), the phosphate group of OPHS is considered to be fixed by Thr-88, Asn-154, Ser-155, Arg-160, and Asn-188 at the active site of TS. The low k_{cat}/K_m values for L-vinylglycine (in the presence of phosphate as well as in the presence of sulfate or in the absence of both phosphate and sulfate; see Table 1) as compared with the corresponding values for OPHS indicate the importance of the phosphate group of OPHS for binding to TS. In contrast to the reaction of L-vinylglycine with TS in the presence of phosphate, the reaction in the presence of sulfate showed a pattern essentially similar to the reaction in the absence of both phosphate and sulfate, *i.e.* only α-ketobutyrate was formed without the formation of L-threonine (Table 1).

The above results indicate that **6** derived from L-vinylglycine is preferentially converted to L-threonine in the presence of phosphate as efficiently as the corresponding reaction for the normal catalysis starting from OPHS, and sulfate cannot substitute for phosphate. To investigate in detail the effect of phosphate ion on the catalytic steps after **6**, we analyzed the "reverse" reaction **1** → **8** → **7** → **6** → **1** starting from L-threonine in the presence of phosphate or sulfate.

Reaction of TS with L-Threonine in the Presence of Phosphate or Sulfate Ion—The addition of L-threonine up to 50 mM to TS caused no spectral changes (supplemental Fig. S1, *A* and *B*). The CD spectrum also showed no detectable changes upon the addition of L-threonine to TS (data not shown). That change in CD is a sensitive indicator of the formation of the external aldimine (19) strongly suggests L-threonine alone cannot form the external aldimine with PLP (**8**) in TS. On the other hand, the addition of phosphate or sulfate to TS slightly increased the 416-nm peak and concomitantly decreased the absorption at around 340 nm (supplemental Fig. S1, *C* and *D*). This indicates that the phosphate or sulfate ion binds to the active site of TS, causing the PLP-Lys-61 aldimine to undergo a tautomeric shift from enolimine to ketoenamine. From the absorption change at 416 nm, the K_d for phosphate and sulfate ions were estimated to be 2.2 and 4.9 mM, respectively.

In the presence of both L-threonine and either of phosphate or sulfate, distinct spectral changes in the TS (supplemental Fig. S1) and α-ketobutyrate formation (Table 2) were observed. However, neither OPHS nor *O*-sulfohomoserine was detected in the reaction mixture (data not shown). This is interpreted to reflect the fact that the step of phosphate elimination (**4** → **5**) is essentially irreversible, and neither phosphate nor sulfate can undergo addition to the Cγ of **5** due to their low Lewis basicities. The kinetic parameters for the α-ketobutyrate formation are summarized in Table 2. The K_d values for phosphate and sulfate kinetically obtained were essentially consistent with the values obtained by the spectro-

scopic measurements described above. The similarity between the K_d values for phosphate and sulfate suggests the similarity of the recognition of the two anions by TS. On the other hand, the k_{cat} and k_{cat}/K_m values in the presence of sulfate were about 7- and 2.4-fold higher, respectively, than those in the presence of phosphate.

Stopped-flow Spectroscopy of the Reaction of TS with L-Threonine—To investigate the reaction steps from L-threonine to α-aminobutyrate in detail, transient kinetic analyses were carried out. A solution containing TS and 50 mM phosphate was reacted with L-threonine (Fig. 1*A*). The absorption at around 330 nm decreased, and that around 410 nm increased within the dead time (2.3 ms), indicating a rapid association of TS and L-threonine. Subsequently, two sharp peaks emerged at 474 and 446 nm, and a broad absorption band at around 330 nm increased. The sharp peaks at 474 and 446 nm are clearly ascribed to the quinonoid intermediate. The absorbance at 331, 416, and 474 nm was plotted *versus* the elapsed time after mixing (Fig. 2*A*). At any wavelengths, the absorbance changes followed a double exponential process, with a k_{app} of ~340 and ~40 s^{-1} at 250 mM L-threonine. These results indicated that the spectral changes in the reaction of TS with L-threonine in the presence of phosphate can be analyzed by a model that includes two steps after the rapid association of the enzyme (*A*) and the substrate (*B*):

$$A + B \underset{}{\overset{K_d}{\rightleftharpoons}} AB \underset{k_{-1}}{\overset{k_{+1}}{\rightleftharpoons}} C \underset{k_{-2}}{\overset{k_{+2}}{\rightleftharpoons}} D \qquad \text{(Eq. 1)}$$

As the rate of α-ketobutyrate formation (k_{cat} = 0.034 s^{-1};

TABLE 2

Kinetic parameters for the α-ketobutyrate formation reaction from L-threonine

TS was incubated with L-threonine in the presence of either phosphate or sulfate, and the solutions were analyzed for α-ketobutyrate (see "Experimental Procedures").

Coexistent anion	K_d for phosphate/sulfate	k_{cat}	k_{cat}/K_m
	mM	s^{-1}	$_M{}^{-1}s^{-1}$
Phosphate	1.7 ± 0.2	0.034 ± 0.002	1.3 ± 0.2
Sulfate	2.6 ± 0.2	0.23 ± 0.04	3.1 ± 0.3

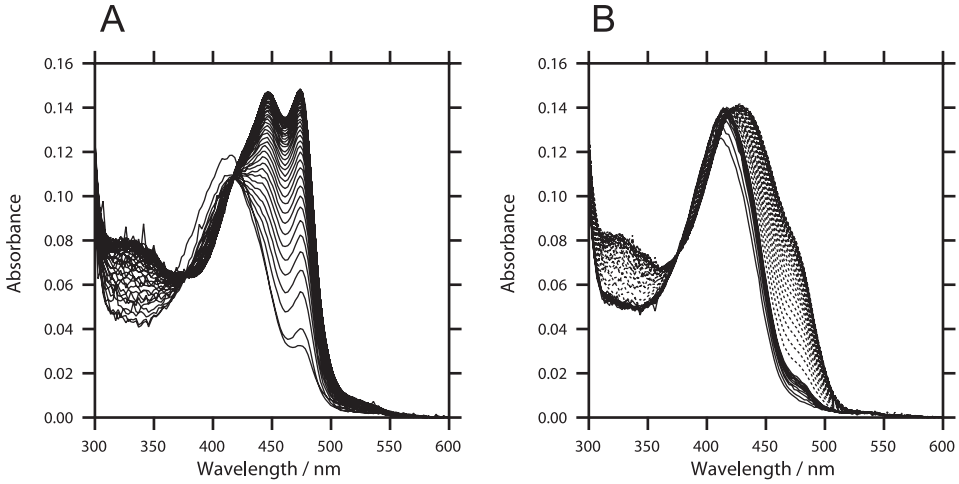

FIGURE 1. **Time-resolved spectra of TS upon reaction with L-threonine in the presence of phosphate (*A*) and sulfate (*B*).** TS (14 μM) in the presence of 50 mM phosphate or sulfate was reacted with 250 mM L-threonine at 298 K in 50 mM PIPES, 100 mM KCl, and 0.1 mM EDTA, pH 8.0, and the spectra were taken at 2.30 (dead time), 3.84 ms, and every 2.56 ms up to 149.76 ms (phosphate) or 4097.28 ms (sulfate). In *panel A* all the spectra are shown. In *panel B* the spectrum at 2.30 ms and those every 12.8 ms between 16.64 and 106.24 ms are shown as *solid lines*, and those every 128 ms between 106.24 and 3946.24 ms are shown as *dotted lines*. In both panels, the spectra with a larger absorption at around 470 nm indicate the spectra at the later times.

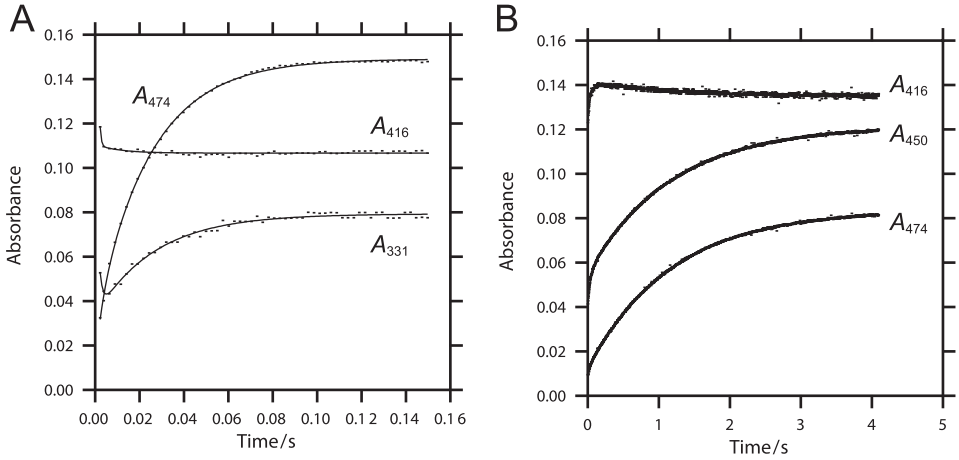

FIGURE 2. **Time course of the absorbance changes in TS upon reaction with 250 mM L-threonine in the presence of phosphate (*A*) and sulfate (*B*).** The wavelength values in nm are indicated in the figure. The experimental values are shown by *dots*, and the theoretical double exponential curves fitted to the experimental values are shown by *solid lines*.

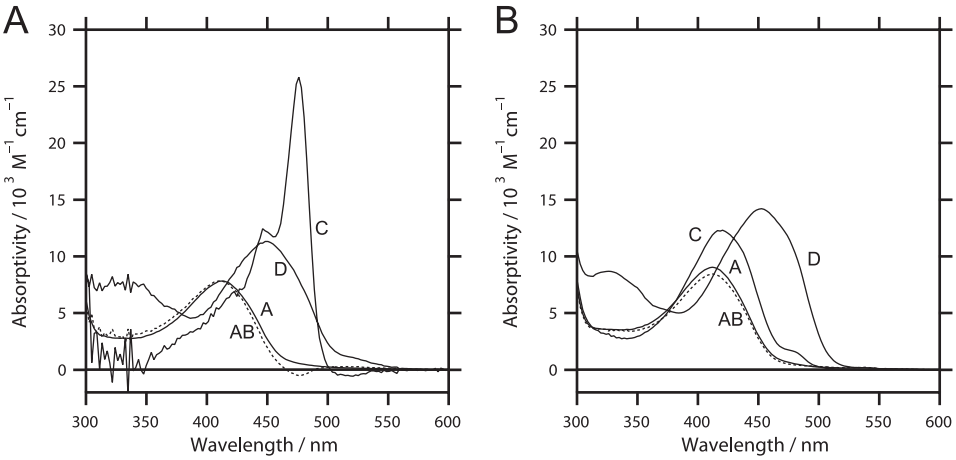

FIGURE 3. **Absorption spectra of the intermediate species obtained from the global analysis of the reaction of TS with L-threonine in the presence of phosphate (*A*) and sulfate (*B*).** The intermediate spectra were obtained from the global fitting analysis of the time-resolved spectra to Equation 1 (in the presence of phosphate) and Equation 2 (in the presence of sulfate). The spectra were assigned to the intermediate species as follows: *A*: *A*, unliganded enzyme; *AB* (*dotted line*), Michaelis complex + external aldimine; *C*, quinonoid intermediate; *D*, PLP-α-aminocrotonate aldimine. *B*: *A*, unliganded enzyme; *AB* (*dotted line*), Michaelis complex; *C*, external aldimine + quinonoid intermediate; *D*, PLP–α-aminocrotonate aldimine. See "Results" for details.

TABLE 3

Transient kinetic parameters for the reaction starting from L-threonine to form α-ketobutyrate

TS was reacted with various concentrations of L-threonine in the presence of either phosphate or sulfate, and the spectral changes were monitored by a stopped-flow spectrophotometer. The time-resolved spectra were subjected to global analysis based on the models of Equation 1 (phosphate) and Equation 2 (sulfate), and the kinetic parameters were obtained. See "Results" for details.

Reaction system	(*E* + phosphate) + L-threonine	(*E* + sulfate) + L-threonine
K_d (mM)	380 ± 2	270 ± 4
k_{+1} (s^{-1})	92 ± 0.4	19 ± 0.5
k_{-1} (s^{-1})	34 ± 1	16 ± 0.1
k_{+2} (s^{-1})	210 ± 4	1.1 ± 0.1
k_{-2} (s^{-1})	66 ± 1	0.053 ± 0.030
k_{+3} (s^{-1})		0.43 ± 0.03

Table 2) is much slower than the k_{app} values of the spectral changes, the regeneration of A from D was not incorporated in this model (Equation 1).

The reaction of TS with L-threonine in the presence of 50 mM sulfate was followed in the same way (Fig. 1*B*). In contrast to the reaction in the presence of phosphate, no significant accumulation of the quinonoid intermediate was observed. The absorption at 416 nm first increased followed by a slow red shift in λ_{max} and an appearance of a shoulder at around 480 nm. The time course of the absorption changes followed a double exponential process (Fig. 2*B*) with k_{app} values of ~30 and ~0.85 s^{-1}. The k_{app} values for the slower spectral changes were of the same order as that of the α-ketobutyrate formation (k_{cat} = 0.23 s^{-1}; Table 2). In this regard, the accumulation of the spectra of the intermediates was apparently lower than that in the presence of phosphate (Fig. 1, *A* and *B*). These results indicate that, contrary to the case in the presence of phosphate, the regeneration of the free enzyme cannot be neglected. Therefore, the spectral changes in the reaction of TS with L-threonine in the presence of sulfate should be analyzed according to the model

$$A + B \underset{}{\overset{K_d}{\rightleftharpoons}} AB \underset{k_{-1}}{\overset{k_{+1}}{\rightleftharpoons}} C \underset{k_{-2}}{\overset{k_{+2}}{\rightleftharpoons}} D \xrightarrow{k_{+3}} A \qquad \text{(Eq. 2)}$$

Global Analysis of the Reaction of TS with L-Threonine—The time-resolved spectra of TS taken after the reaction with various concentrations (10, 20, 50, 80, 120, 160, 200, and 250 mM) of L-threonine were subjected to a global fitting analysis using the models of Equation 1 (reactions in the presence of phosphate) and 2 (reactions in the presence of sulfate). For the initial values of the kinetic parameters, the apparent rate constants obtained from the double exponential fitting (Fig. 2) were divided by 2, assuming the equilibrium constant of 1 for [AB]/[C] and [C]/[D], and were used for k_{+1}, k_{-1}, k_{+2}, and k_{-2}. For the initial values of K_d, the K_m values for L-threonine calculated from the k_{cat} and k_{cat}/K_m values (Table 2) were used. After the fitting, the spectra of TS and the intermediates, *i.e.* A, AB, C, and D, and the kinetic parameters were obtained, each summarized in Fig. 3 and Table 3, respectively.

For both reactions in the presence of phosphate and sulfate, the spectra of the intermediate D showed a large absorption band at 450 nm and a smaller one at around 330 nm. These spectra of D resemble those of the PLP-α-aminoacrylate aldimine reported for several enzymes in the absorption maxima, strength, and shape (20–22). Considering the same conjugate system between the PLP–α-aminoacrylate aldimine and the PLP-α-aminocrotonate aldimine, we can conclude that D is the PLP-α-aminocrotonate aldimine (**6**), whose ketoenamine and enolimine tautomers absorb at 450 and 330 nm, respectively.

For the reaction in the presence of phosphate, the intermediate C showed the typical spectrum of the quinonoid intermediate (Fig. 3*A*) and was attributed to **7**. Accordingly, the spectrum of the intermediate AB, which was similar to that of A, was considered to be that of the Michaelis complex with L-threonine (not shown in Scheme 1 but exists between **8** and **1**), the external aldimine (**8**), or both. On the other hand, for the reaction in the presence of sulfate ion, the spectra of the intermediate C showed a large absorption band at 420 nm and a faint absorption band at around 480 nm (Fig. 3*B*). The shape and the position of the spectrum showed that the intermediate C is largely the PLP aldimine with no double bond in the

substrate moiety conjugated to the imine. As compared with the absorption band of AB, which was again similar to A, the absorption band of C was red-shifted (~8 nm) and had a larger intensity at 420 nm and a smaller one at 330 nm. This indicates that AB and C are both PLP aldimines but are clearly distinguished. The most probable interpretation is that AB and C are the Michaelis complex with L-threonine and the external aldimine (**8**), respectively. Spectral changes similar to this are observed in the transaldimination process of a number of PLP enzymes (19). Assuming that the Michaelis complex and the external aldimine in the reaction in the presence of phosphate have similar absorption spectra as those in the reaction in the presence of sulfate, the absorption spectrum of AB in the presence of phosphate indicates that it is mainly composed of the Michaelis complex.

The presence of a small absorption at around 480 nm in the spectrum of C in the presence of sulfate suggests the presence of a trace amount of the quinonoid intermediate (Fig. 3*B*). Using the ϵ value at 476 nm of C in the presence of phosphate (Fig. 3*A*), the fraction of the quinonoid intermediate in C in the presence of sulfate was estimated to be 6.7%. We could not resolve C by global fitting based on the model of a three-step process after the Michaelis complex. This indicates that in the presence of sulfate the concentrations of the external aldimine and the quinonoid intermediate change in parallel, showing that the process of the interconversion between the external aldimine (**8**) and the quinonoid intermediate (**7**) is considerably fast when compared with the other processes.

Comparison of the Steady-state and Transient Kinetic Parameters for L-Threonine—The steady-state and the transient kinetic parameters are related to each other by the following equations:

$$k_{cat} = \frac{1}{\frac{1}{k_{+1}} + \frac{k_{-1}}{k_{+1}}\frac{1}{k_{+2}} + \frac{k_{-1}}{k_{+1}}\frac{k_{-2}}{k_{+2}}\frac{1}{k_{+3}} + \frac{1}{k_{+2}} + \frac{k_{-2}}{k_{+2}}\frac{1}{k_{+3}} + \frac{1}{k_{+3}}} \quad \text{(Eq. 3)}$$

$$\frac{k_{cat}}{K_m} = \frac{1}{\left(\frac{1}{k_{+1}} + \frac{k_{-1}}{k_{+1}}\frac{1}{k_{+2}} + \frac{k_{-1}}{k_{+1}}\frac{k_{-2}}{k_{+2}}\frac{1}{k_{+3}}\right)K_d} \quad \text{(Eq. 4)}$$

where the microscopic kinetic parameters are those shown in Equations 1 and 2. For the reaction in the presence of phosphate, the k_{+3} value was the only undetermined value. This was calculated to be 0.049 s^{-1} using Equation 3 and the observed k_{cat} value for the reaction with L-threonine in the presence of phosphate.

Now that the microscopic kinetic parameters have been obtained, we can estimate the steady-state kinetic parameters k_{cat} and k_{cat}/K_m using Equations 3 and 4. The k_{cat}/K_m value was 1.1 $M^{-1}s^{-1}$ in the presence of phosphate, and k_{cat} = 0.23 s^{-1} and k_{cat}/K_m = 4.0 $M^{-1}s^{-1}$ in the presence of sulfate. The calculated values excellently matched the observed values (Table 2), showing the validity of the kinetic analysis described above.

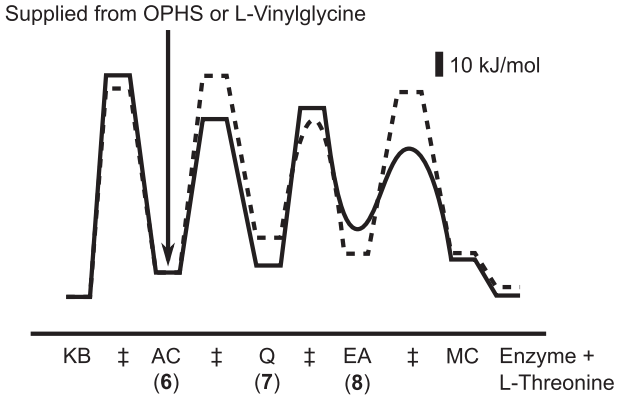

FIGURE 4. **Free energy profiles of the catalytic reaction of TS after the PLP-α-aminocrotonate aldimine in the presence of phosphate (*solid line*) and sulfate (*dashed line*).** The energy levels of the two profiles are adjusted at the PLP-α-aminocrotonate aldimine. The kinetic parameters obtained from the reaction of TS with L-threonine in the presence of phosphate or sulfate were used for calculating the free energy levels. The equations used are: $k = (k_BT/h)\exp((-\Delta G^{\ddagger})/RT)$ for the transition states $K_{eq} = \exp(-\Delta G/RT)$ for the free energy difference between the two states in equilibrium. The energy levels of E + L-threonine are those when [L-threonine] = 1 mM, and those of KB are arbitrary. The *curved portions of the lines* indicate that these energy levels are not quantized. For the free energy profile in the presence of phosphate, the energy level of the transition state (‡) between *EA* and *MC* is lower than that between *Q* and *EA*, and the energy level of EA is significantly higher than that of *MC*. For the free energy profile in the presence of sulfate, the energy level of ‡ between *Q* and *EA* is significantly lower than that between *EA* and *MC*. Abbreviations are: *KB*, TS + NH_3 + α-ketobutyrate; *AC*, PLP-α-aminocrotonate aldimine; *Q*, quinonoid intermediate; *EA*, external aldimine of TS with L-threonine; *MC*, Michaelis complex of TS with L-threonine.

Free-energy Profile of the Steps of the Latter Part of the TS Catalytic Reaction—Using the microscopic kinetic parameters obtained above, the free energy profile of the reaction steps between L-threonine and α-ketobutyrate could be obtained. The energy profiles in the presence of phosphate and sulfate are shown in Fig. 4. The profiles were drawn according to the direction of the normal catalytic steps shown in Scheme 1. Uncertainties about the energy levels of several intermediates and transition states arising from the inability to dissect the reaction steps are also shown. The profiles indicate that, in the presence of phosphate as compared with sulfate, the transition state between the PLP-α-aminocrotonate aldimine (**6**) and the quinonoid intermediate (**7**) and that between the external aldimine (**8**) with L-threonine and the Michaelis complex with L-threonine are stabilized (Fig. 4). For the transition state between the PLP–α-aminocrotonate aldimine (**6**) and the quinonoid intermediate (**7**), the stabilization energy was calculated to be 17.7 kJ·mol^{-1}, corresponding to the rate enhancement of about 10^3.

Crystal Structure of TS Complexed with a Structural Analog for the PLP-α-Aminocrotonate Aldimine—**10** (Fig. 5*B*), which is a condensation product of PLP and pyruvic acid, has been used as an analog for the PLP-α-aminoacrylate aldimine in serine dehydratase (11). Because of the structural similarity of the PLP-α-aminoacrylate aldimine and the PLP-α-aminocrotonate aldimine as described above, we expected that **10** can also be used as an analog for the PLP-α-aminocrotonate aldimine (**6**) in TS. The apoenzyme of TS was reconstituted with **10** and crystallized in the presence of phosphate. Crystallization of the relevant structures, such as TS, TS complexed with

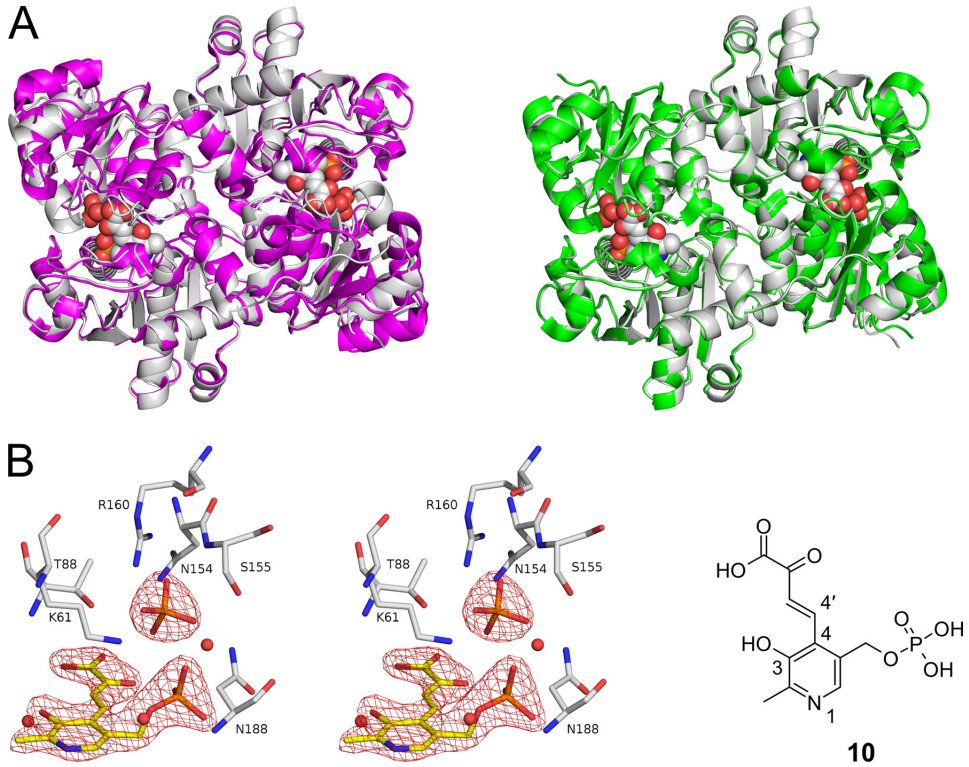

FIGURE 5. *A*, the overall structure of TS obtained by x-ray crystallography is shown. *Left*, overlay of TS complexed with **10** (*gray*) and the unliganded holoenzyme of TS (*magenta*; PDB code 1UIM, 8). *Right*, overlay of TS complexed with **10** (*gray*) and TS complexed with AP5 (*green*; PDB code 1V7C, 8). In both structures, only **10** and the bound phosphate ion are shown in the sphere models for clarity. *B*, the $F_o - F_c$ omit map of TS complexed with **10**, contoured at 5σ. The chemical structure of **10** is shown with the atomic numbering.

10, and the apoenzyme of TS either in the phosphate- or sulfate-bound form has been attempted. However, only the crystals of the apoenzyme of TS complexed with sulfate (apoTS-S) were obtained so far. The structures of TS-10-P and apoTS-S were determined by x-ray crystallography at 2.10 and 1.92 Å resolutions, respectively (Table 4). The overall structure of TS-10-P is shown in Fig. 5*A* and compared with the structures of TS and TS complexed with AP5 (TS-AP5) (Fig. 5*A*). The structure of apoTS-S was superimposable on that of TS, showing that the enzyme does not undergo any global conformational change upon the binding of PLP (supplemental Fig. S2*A*). However, the binding of the substrate analog AP5 to the holoenzyme induces a large conformational change from the open to the closed form in which the small domain of TS moves as a rigid body to close the active site (8). This closed structure was maintained in TS-10-P (Fig. 5*A*), indicating that TS is in the closed form in the enamine and the PLP-α-aminocrotonate aldimine intermediates. These data support the catalytic model that TS is in the closed form, whereas the substrate and the intermediates are bound to the enzyme.

Phosphate Ion Bound to the Active Site—The $F_o - F_c$ omit map clearly showed an electron density of **10** in the active site (Fig. 5*B*). The modeled structure of **10** was almost completely planar, reflecting that all the C atoms of **10** except for C2′ and C5′ are sp^2-hybridized. In addition to this electron density, a distinct electron density having a tetrahedral shape was observed. A phosphate ion could be excellently fit to this density, indicating that a phosphate ion derived from the solvent is bound to the active site of TS-10-P (Fig. 5*B*). It is important to confirm that this is not a sulfate ion that has been used to prepare the apoenzyme. The solution used for crystallization contained less than 5 pmol of sulfate ion (1 μM × 5 μl, see "Experimental Procedures"). The number of the cells in a single crystal is estimated to be 1.5×10^{12} as calculated from the size of the crystal and the unit cell dimensions. Because there

TABLE 4
Statistics of data collection and crystallographic refinement

	apoTS-S	TS-10-P
Data collection		
Temperature (K)	100	100
Wavelength (Å)	0.9	0.9
Space group	$P3_221$	$P3_221$
Unit cell dimensions, *a*, *b*, *c* (Å)	113.0, 113.0, 150.3	115.2, 115.2, 99.7
No. of observations	929,780	525,702
No. of unique reflections	164,186	92,864
Multiplicity	5.7 (5.3)	5.7 (5.2)
$d_{max} - d_{min}$ (Å)	50-1.92 (1.95-1.92)	50-2.05 (2.09-2.05)
Overall completeness (%)	100 (100)	100 (100)
Overall R_{merge} (%)[a]	6.3 (50.6)	8.3 (72.1)
Refinements statistics		
$d_{max} - d_{min}$ (Å)	48.9-1.92	26.6-2.10
Residues in the core $\varphi\psi$ region (%)	90.3	89.2
No. of solvent atom	599	272
Root mean square deviation from ideal values		
Bond lengths (Å)	0.005	0.006
Bond angles (degrees)	1.2	1.44
Residual *R* (%)[b]	22.7	21.6
Free residual *R* (%)[c]	26.0	25.3
Fraction of data in R_{free} set (%)	5	5

[a] $R_{merge} = \Sigma_h\Sigma_i|I_{hi} - \langle I_h\rangle|/\Sigma_h\Sigma_i I_{hi}$, where I_{hi} is the intensity value of the *i*th measurement of *h*, and $\langle I_h\rangle$ is the corresponding mean value of I_h for all *i* measurements.
[b] $R = \Sigma||F_o| - |F_c||/\Sigma|F_o|$.
[c] Free residual *R* is an *R* factor of the CNS refinement evaluated for 5% of reflections that were excluded from the refinement. Values in parentheses refer to the highest resolution shell.

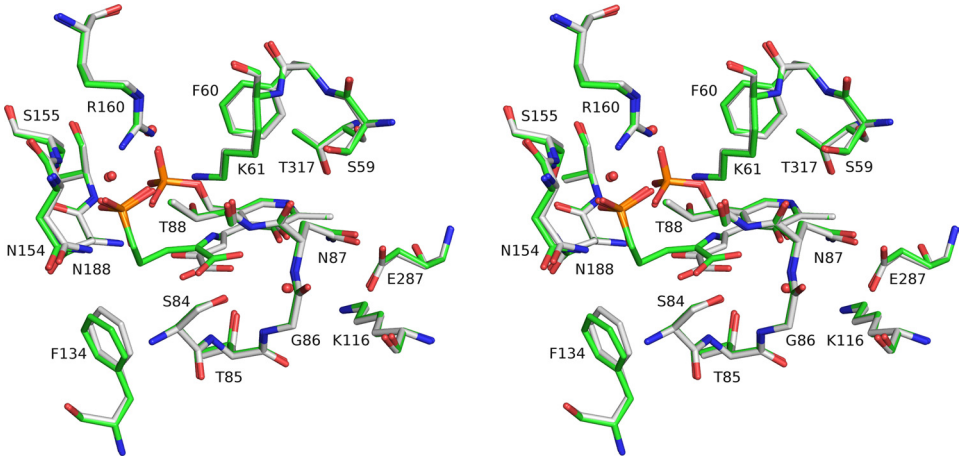

FIGURE 6. **Overlay of the structures of TS complexed with 10 and phosphate ion (TS-10-P) and AP5 (TS-AP5).** The carbon atoms of TS-10-P and TS-AP5 are shown in *gray* and *green*, respectively. The α-carbon atoms of the active site residues shown in this figure of subunit B of TS-10-P and subunit C of TS-AP5 were fitted by root mean square minimization. For details of the hydrogen bond and other interactions, refer to "Results."

were at least 10 crystals of a size similar to this, the "amount" of the active sites in the crystals are calculated to be more than 50 pmol. Therefore, even if all the sulfate ions remaining in the solution are bound to the crystals, it can occupy less than 10% of the active sites. From these calculations we consider that the observed tetrahedral electron density comes from the bound phosphate ion.

The active site structure of TS-10-P was superimposed on that of TS-AP5 (Fig. 6). The PLP moiety of TS-AP5 and that of TS-10 reside in the same plane. However, in contrast to the planar conformation of **10**, C4′ and Nα of TS-AP5 are sp^3-hybridized. As a result, the Cα of **10** of TS-10-P deviates from the corresponding Cα of TS-AP5 by 0.4 Å, with a clockwise 21° rotation (viewed from the *Re* face of AP5, *i.e.* the *Si* face of **10**, Cα being taken as the prochiral center) of the three bonds around Cα about the axis passing through Cα and perpendicular to the plane of **10**. Consequently, the position of the carboxylate group is substantially different from that of AP5. Nevertheless, the carboxylate group of **10** and that of AP5 make hydrogen bonds with the same neighboring groups (Fig. 6), *i.e.* the main chain NH groups of Thr-85, Asn-87, and Thr-88, the side chain OH group of Ser-84, and a water molecule.

The phosphate ion in TS-10-P is located at exactly the same position as the phosphono group of AP5 in TS-AP5 and is stabilized by interaction with the same groups, *i.e.* the side chains of Lys-61, Thr-88, Asn-154, Ser-155, Arg-160, and Asn-188 (Fig. 6). The only difference between the phosphate ion and the phosphono group is the possible presence of a hydrogen bond between the carboxylate group of **10** and an O atom of phosphate, which is replaced by a C atom in AP5 (Fig. 6).

The crystal structure of apoTS-S showed that the cavity formed by the removal of PLP is filled with three water molecules and two sulfate ions derived from the solvent (supplemental Fig. S2*B*). One of the sulfate ions is located at the same position, albeit with an ~30° rotation, as the phosphate group of **10** in TS-10-P and that of PLP in the holoenzyme. Another sulfate ion interacts with the ϵ-amino group of Lys-61, a water molecule, and the main chain NH group of Asn-87, which is the residue that interacts with the carboxylate group of **10** in TS-10-P (supplemental Fig. S2*B*). A third sulfate ion forms hydrogen bonds with the side chains of Thr-88, Arg-160, and Asn-188 and a water molecule. These residues are involved in the binding of the phosphate ion in TS-10-P, and as the result, the sulfate ion is located at a position close to that of the phosphate ion in TS-10-P (supplemental Fig. S2*B*). The deviation in the position of the sulfate ion is considered to be due to the open conformation of the enzyme protein. Although the crystal structure of TS complexed with **10** and the sulfate ion has not been obtained, these data strongly suggest that the sulfate ion binds to the same position as the phosphate ion during the course of catalysis by TS.

DISCUSSION

Reaction Specificity of PLP Enzymes and TS—PLP catalyzes versatile reactions of amino acids, such as racemization, transamination, elimination, replacement, decarboxylation, aldol cleavage, etc. This indicates that a PLP enzyme must be organized to carry out a specific type of reaction. An important mechanism that accounts for the reaction specificity of the PLP enzymes has been provided by the Dunathan hypothesis (23), which suggests that the conformation of the external aldimine at the active site determines the reaction type; if the bond perpendicular to the plane of the imine-pyridine ring is C-H, C-COO^-, or C-CHOH-, then α-deprotonation, decarboxylation, or aldol cleavage occurs, respectively. Although this crucially determines the reaction during the early step of the catalysis, this alone cannot explain all of the reaction specificity of the PLP enzymes. For example, there are many types of reactions that start with α-deprotonation, such as racemization, transamination, β-elimination, β-replacement, γ-elimination, γ-replacement, etc. The individual PLP enzymes catalyzing only one of those reactions must control the proton transfer processes to realize their reaction specificity.

TS is a unique PLP enzyme undergoing γ-elimination and β-addition reactions. Therefore, TS shares the reaction pathway **1**–**6** with γ-lyases, and this distinguishes them from γ-synthases, which do not catalyze the step between **5** and **6**, the proton transfer between C4′ and Cγ. However, TS is different from the γ-lyases in that it preferentially catalyzes the

addition of water at the Cβ of **6** as compared with the transaldimination of **6** to yield α-ketobutyrate (Table 1). Therefore, it is important to know how TS controls these steps to carry out the specific biosynthetic reaction.

*Phosphate Ion Promotes the Reaction Steps from **6** to L-Threonine*—In this study it was shown that L-vinylglycine, which has been known to be an alternate substrate for the γ-synthase (24, 25) and 1-aminocycleopropane-1-carboxylate synthase (26) reactions, can be incorporated into and processed at the active site of TS (Table 1). In the presence of phosphate ion, TS forms L-threonine from L-vinylglycine with a k_{cat} value and a reaction specificity comparable with those when OPHS was used as the substrate (Table 1). However, in the absence of phosphate ion or in the presence of sulfate ion, only α-ketobutyrate was formed (Table 1). These results indicated that the phosphate ion accelerates the reaction from **6** to the L-threonine formation, and this function is related to a property of the phosphate ion, which is absent in the sulfate ion.

*Phosphate as a Base Catalyst for the Addition of Water at the Cβ of **6***—To clarify the function of the phosphate ion in the L-threonine formation reaction in detail, the reverse reaction starting from L-threonine was kinetically studied in the presence of phosphate or sulfate. The result showed that the phosphate ion lowers the energy barrier for the addition of the water molecule at the Cβ of **6** and the transaldimination to form L-threonine, as compared with the sulfate ion (Fig. 4). Therefore, we structurally studied how the phosphate ion is involved in the reactions starting from **6** by solving the crystal structure of TS complexed with an analog for **6** (Fig. 5). The phosphate ion was found to bind to the site originally occupied by the phosphate group of OPHS and was supposed to interact with the attacking water molecule in the step **6** → **7**. The energy barrier for this step in the absence of phosphate or sulfate was not obtained because of the extremely low affinity of L-threonine in the absence of phosphate or sulfate. However, the finding that the phosphate ion lowers the energy barrier more effectively than the sulfate ion, which has a much lower basicity (pK_a = 1.92 *versus* 7.21; values for the second dissociation at 298 K), strongly indicates that the phosphate acts as a base catalyst during the attack of water on the Cβ of **6**. From the difference in the pK_a values and the rate constants, the Brønsted β was estimated to be 0.59, indicating that the proton is in an intermediate position between the O atoms of the attacking water molecule and the phosphate or sulfate at the transition state.

In contrast to the effect on the step of the addition of water at Cβ, the effect of phosphate ion on the transaldimination **8** → **1** is more difficult to understand. We will return to this problem later.

Possible Involvement of the Phosphate Ion in the Protonation/Deprotonation at Cγ—That the phosphate ion locates near the Cγ of **6** and is the base catalyst for the addition of the water molecule to Cβ raises the possibility that this phosphate ion is also involved in the protonation/deprotonation at Cγ, as we have suggested in a previous crystallographic study on TS complexed with AP5 (8). This conjecture is attractive as the ε-amino group of Lys-61 is too distant from Cγ and other

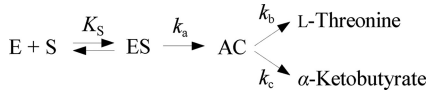

SCHEME 2

group(s) are considered to be required to protonate/deprotonate the atom. Using the kinetic parameters obtained in this study, we estimated the effect of phosphate on this step as follows.

A simple mechanism for the reaction starting from L-vinylglycine is Scheme 2, where E, S, and AC denote the enzyme, L-vinylglycine, and the PLP-α-aminocrotonate aldimine (**6**), respectively. Using the above simple mechanism, the k_{cat} values for L-threonine and α-ketobutyrate formation are expressed as,

$$k_{cat}^{L\text{-}threonine} = \frac{k_a k_b}{k_a + k_b + k_c} \quad \text{(Eq. 5)}$$

$$k_{cat}^{\alpha\text{-}ketobutyrate} = \frac{k_a k_c}{k_a + k_b + k_c} \quad \text{(Eq. 6)}$$

The ratio of these k_{cat} values is equal to k_b/k_c and was calculated to be 47 in the presence of phosphate (Table 1). Therefore, using the value of k_c = 0.049 s^{-1} (k_c is equal to k_{+3}, which in the presence of phosphate is estimated to be 0.049 s^{-1}; see the calculation shown after Equations 3–4), k_a was estimated to be 0.85 s^{-1} from Equation 5.

In the absence of phosphate, on the other hand, Equation 6 is simplified to

$$k_{cat}^{\alpha\text{-}ketobutyrate} = \frac{k_a k_c}{k_a + k_c} \quad \text{(Eq. 7)}$$

This has a value of 0.015 s^{-1} (Table 1). As the PLP-α-aminocrotonate aldimine was not detected in the reaction of TS with L-vinylglycine (supplemental Fig. S3*B*), k_a is apparently smaller than k_c and should be almost equal to the k_{cat} value, 0.015 s^{-1}. Therefore, we can consider that k_a is increased 57-fold in the presence of phosphate.

In the presence of sulfate, k_c = 0.43 s^{-1} (equal to k_{+3}; Table 3). Therefore, k_a is almost equal to the k_{cat} value of 0.0034 s^{-1} (Table 1). This is even lower than the k_a in the absence of phosphate or sulfate (0.015 s^{-1}; see above), indicating that the sulfate ion, unlike the phosphate ion, does not have the ability to enhance k_a.

Altogether, these calculations indicate that phosphate promotes the step **9** → **6**, probably by functioning as an acid-base catalyst. The rate enhancement (57-fold) is moderate as compared with the value (10^3-fold) for the addition of water at Cβ. The remaining reaction in the absence of phosphate may be ascribed to the catalysis by water molecule(s) near Cγ.

The step **9** → **6** is a nonphysiological reaction that exists on the way from the unnatural substrate L-vinylglycine. However, considering the similarity in the reaction (protonation at Cγ), we can expect that the phosphate ion functions in the same way in the step **5** → **6** during the normal catalysis.

Effect of Phosphate Ion on the Transaldimination Steps—One of the problems concerning the reaction specificity of TS

is the two transaldimination processes starting from **6** and **8**. Ideally, the former should be inhibited, and the latter should be promoted during the catalytic reaction of TS. It is, then, important to know the effect of the phosphate ion on these steps. However, as the rate constant for neither of these steps in the absence of phosphate or sulfate could be obtained, the effect of the phosphate ion can be discussed only in comparison with the effect of the sulfate ion.

The rate constant for the transaldimination from **6** is 9-fold higher in the presence of the sulfate ion (Table 3 and the estimated value of $k_{+3} = 0.049\ s^{-1}$ in the presence of phosphate), whereas the rate constant for the transaldimination from **8** is higher in the presence of phosphate. The difference between the structure of **6** and **8** is the presence (**8**) or absence (**6**) of the β-OH group and the hybridization at Cα (sp^2 for **6** and sp^3 for **8**). As the phosphate ion can interact with both the β-OH group and the ϵ-amino group of Lys-61 and the latter is the group that directly involved in the transaldimination process, the presence/absence of the β-OH group may affect the transaldimination process. As a simple hypothesis, assuming that the β-OH group and the ϵ-amino group of Lys-61 compete with each other for binding to the phosphate ion, we can expect that the ϵ-amino group forms a hydrogen bond with the phosphate ion in **6**, as observed in the crystal structure of TS-10-P (Fig. 5) but is liberated from the phosphate ion in **8**. This may result in attenuating the transaldimination of **6** without affecting the transaldimination of **8**. The reverse effect of the sulfate ion may be ascribed to the absence of protons in the sulfate ion.

Product-assisted Catalysis—As shown in the structure of TS-10-P, the phosphate ion is stabilized by many residues at the active site. This is considered to be the cause of the fairly high affinity of the phosphate ion to TS ($K_d = 2.2$ mM). However, comparison of the structure of the unliganded enzyme and TS-10-P indicates that, among the residues interacting with the phosphate ion in TS-10-P, Thr-88, Asn-154, and Ser-155 move toward the phosphate ion upon the conformational change from the open to the closed structure induced by the substrate binding. Therefore, it is expected that during the catalysis the phosphate ion has a much higher affinity to the enzyme than that to the unliganded enzyme. The phosphate ion released at the step of **4** → **5** is then considered to remain at the active site and acts as the catalytic base that directs the reaction from **6** toward the formation of L-threonine.

The product-assisted catalysis in the enzyme has been reported for human 8-oxoguanine DNA glycosylase/lyase (27). The enzyme cleaves 8-oxoguanine from DNA and uses it as a catalyst for the following steps. Although the reactions catalyzed by TS and 8-oxoguanine DNA glycosylase/lyase are different, both reactions are complex and involve many elementary steps. Therefore, during the evolution, these enzymes may have adopted a strategy to expand their catalytic potential by incorporating the product as the catalytic species.

One of the reasons for the presence of the phosphate group in the natural substrate OPHS is to provide a good leaving group at Cγ. However, as shown in this study, the released phosphate in turn functions as the catalyst in the subsequent steps, and this mechanism explains how the reaction is controlled in TS at the branching point (**6**) of the catalysis dividing the β-synthase and the γ-lyase. Although this is a crucial element that warrants the reaction specificity of TS, the catalytic reaction of TS contains other branching points that are subject to side reactions unless there are mechanisms to control the pathway. These points should be studied in the future.

REFERENCES

1. Flavin, M., and Slaughter, C. (1960) *J. Biol. Chem.* **235,** 1112–1118
2. Alexander, F. W., Sandmeier, E., Mehta, P. K., and Christen, P. (1994) *Eur. J. Biochem.* **219,** 953–960
3. Hayashi, H., (1995) *J. Biochem.* **118,** 463–473
4. Laber, B., Maurer, W., Hanke, C., Gräfe, S., Ehlert, S., Messerschmidt, A., and Clausen, T. (1999) *Eur. J. Biochem.* **263,** 212–221
5. Covarrubias, A. S., Högbom, M., Bergfors, T., Carroll, P., Mannerstedt, K., Oscarson, S., Parish, T., Jones, T. A., and Mowbray, S. L. (2008) *J. Mol. Biol.* **381,** 622–633
6. Garrido-Franco, M., Ehlert, S., Messerschmidt, A., Marinkovic', S., Huber, R., Laber, B., Bourenkov, G. P., and Clausen, T. (2002) *J. Biol. Chem.* **277,** 12396–12405
7. Thomazeau, K., Curien, G., Dumas, R., and Biou, V. (2001) *Protein Sci.* **10,** 638–648
8. Omi, R., Goto, M., Miyahara, I., Mizuguchi, H., Hayashi, H., Kagamiyama, H., and Hirotsu, K. (2003) *J. Biol. Chem.* **278,** 46035–46045
9. Laber, B., Gerbling, K. P., Harde, C., Neff, K. H., Nordhoff, E., and Pohlenz, H. D. (1994) *Biochemistry* **33,** 3413–3423
10. Toney, M. D., and Kirsch, J. F. (1993) *Biochemistry* **32,** 1471–1479
11. Schnackerz, K. D., Ehrlich, J. H., Giesemann, W., and Reed, T. A. (1979) *Biochemistry* **18,** 3557–3563
12. Madsen, B. C., and Murphy, R. J. (1981) *Anal. Chem.* **53,** 1924–1926
13. Möckel, B., Eggeling, L., and Sahm, H. (1992) *J. Bacteriol.* **174,** 8065–8072
14. Otowinowski, Z., and Minor, W. (1997) *Methods Enzymol.* **276,** 307–326
15. Collaborative Computational Project Number 4 (1994) *Acta Crystallogr. D Biol. Crystallogr.* **50,** 760–763
16. Brünger, A. T., Adams, P. D., Clore, G. M., DeLano, W. L., Gros, P., Grosse-Kunstleve, R. W., Jiang, J. S., Kuszewski, J., Nilges, M., Pannu, N. S., Read, R. J., Rice, L. M., Simonson, T., and Warren, G. L. (1998) *Acta Crystallogr. D Biol. Crystallogr.* **54,** 905–921
17. McRee, D. E. (1999) *J. Struct. Biol.* **125,** 156–165
18. Kleywegt, G. J., and Jones, T. A. (1997) *Methods Enzymol.* **277,** 208–230
19. Ikushiro, H., Hayashi, H., and Kagamiyama, H. (2004) *Biochemistry* **43,** 1082–1092
20. Jhee, K. H., Niks, D., McPhie, P., Dunn, M. F., and Miles, E. W. (2001) *Biochemistry* **40,** 10873–10880
21. Hur, O., Niks, D., Casino, P., and Dunn, M. F. (2002) *Biochemistry* **41,** 9991–10001
22. Karsten, W. E., and Cook, P. F. (2002) *Methods Enzymol.* **354,** 223–237
23. Dunathan, H. C. (1966) *Proc. Natl. Acad. Sci. U.S.A.* **55,** 712–716
24. Johnston, M., Marcotte., P., Donovan, J., and Walsh, C. (1979) *Biochemistry* **18,** 1729–1738
25. Esaki, N., Suzuki, T., Tanaka, H., Soda, K., and Rando, R. R. (1977) *FEBS Lett.* **84,** 309–312
26. Feng, L., and Kirsch, J. F. (2000) *Biochemistry* **39,** 2436–2444
27. Fromme, J. C., Bruner, S. D., Yang, W., Karplus, M., and Verdine, G. L. (2003) *Nat. Struct. Biol.* **10,** 204–211

Enzymology:

Product-assisted Catalysis as the Basis of the Reaction Specificity of Threonine Synthase

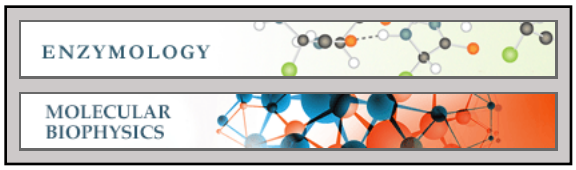

Takeshi Murakawa, Yasuhiro Machida and Hideyuki Hayashi

J. Biol. Chem. 2011, 286:2774-2784.
doi: 10.1074/jbc.M110.186205 originally published online November 17, 2010
